

# Film thickness and roughness of ZDDP antiwear films

Ksenija Topolovec-Miklozic<sup>a</sup>, T. Reg Forbus<sup>b</sup> and Hugh A. Spikes<sup>a,\*</sup>

<sup>a</sup>Imperial College London, London, UK

<sup>b</sup>Ashland, Inc., Lexington, KY, USA

Received 20 September 2006; accepted 11 December 2006; published online 9 January 2007

The two experimental techniques, spacer layer interferometry imaging (SLIM) and atomic force microscopy (AFM), have been used to measure the thickness and roughness of zinc dialkyl dithiophosphate (ZDDP) reaction films formed in a rolling-sliding minitraction machine (MTM) tribometer. The AFM method has been complemented by a novel ZDDP film removal method based on ethylenediaminetetraacetic acid (EDTA) solution. It has been found that the two approaches measure very similar ZDDP film thickness values, lending credence to both methods. However the AFM approach measures much rougher ZDDP reaction films than MTM-SLIM and it is believed that SLIM underestimates the film roughness. Based on this, the use of MTM-SLIM is recommended for monitoring the evolution of antiwear film thickness during rubbing, while AFM should be employed for studying the morphology of antiwear films.

**KEY WORDS:** zinc dialkyldithiophosphate, ZDDP, film, boundary lubrication, thickness, roughness, antiwear

## 1. Background

There has been a great deal of research to characterize the reaction films formed by the antiwear additive zinc dialkyl dithiophosphate (ZDDP). Particular attention has focused on the thickness of ZDDP films since it is known that thick ZDDP surface films enhance mixed lubrication friction [1] and influence wear [2].

In practice, ZDDP film thickness is difficult to quantify precisely since ZDDP forms patchy, uneven reaction films. It is thus important to represent film thickness by more than a single value: the maximum and mean film thickness, the kinetics of the film thickness, the root mean square roughness and average slope are all likely to be important.

Measurements of the thickness of antiwear films formed by ZDDP solutions on rubbing surfaces published over more than the last 50 years agree surprisingly well, despite the fact that the ZDDP films studied were formed in different rubbing experiments and that various film thickness characterization methods were employed.

Soon after ZDDPs were introduced as lubricant additives it was recognized that they form relatively thick films on rubbed surfaces compared to most other lubricant additives. In the 1950s, <sup>32</sup>P radiotracing was used to show that ZDDP solutions rapidly formed films on rubbed cast iron surfaces that stabilized at approximately 120 nm thickness [3]. Using X-ray fluorescence

(XRF) Rounds [4] found that films formed by ZDDP on rubbed surfaces were ‘several hundred monolayers thick’.

The development of vacuum-based surface analysis techniques in the 1970s, such as X-ray photoelectron spectroscopy (XPS), Auger Electron Microscopy (AES) and Secondary Ion Mass Spectroscopy (SIMS) with successive ion etching enabled both the composition and film thickness of ZDDP films to be measured. The overall film thickness of the film was estimated to be about 1000 monolayers [5] or 50–100 nm [6].

Electrical contact resistance (ECR) measurements were also employed to show the formation of insulating ZDDP reaction films. Georges et al. [5] studied the induction period prior to ZDDP forming an insulating reaction film and observed the temperature-dependent formation of a “thick” film in a steel-on-steel rubbing contact. ECR has been used by many other authors to monitor the generation of insulating film between rubbed surfaces with broadly similar findings [6–10]. Until recently this was the only method that could continually monitor film thickness within the rubbing contact while rubbing itself is taking place, but unfortunately this technique does not provide a reliable measure of actual film thickness as there is no direct relationship between contact resistance and film thickness.

In the 1980s, as analytical instruments became more sensitive, more detailed information could be obtained on the thickness of ZDDP reaction films. Palacios used Energy Dispersive X-ray Analysis (EDAX) to carry out film thickness determination of the ZDDP tribofilm

\*To whom correspondence should be addressed.  
E-mail: h.spikes@imperial.ac.uk

formed under varying load, rubbing time and ZDDP concentration and found that ZDDP formed films up to 140 nm thick [2, 11].

Choa et al. [12] used ellipsometry to monitor film thickness and refractive index of ZDDP boundary films formed during rubbing over a range of temperature. At low to moderate loads, high temperatures and high concentrations of ZDDP a thick film of 80 nm was rapidly established.

In 2000, X-Ray Absorption Near Edge Structure (XANES), a technique primarily used to provide P and S bonding information in ZDDP tribofilms, was also shown to be capable of monitoring the thickness of these films [13]. Zhang et al. [14] monitored ZDDP reaction film thickness with rubbing time and showed that the thickness of ZDDP films increased up to 100 nm in the first hour of rubbing, after which it decreased to eventually level out during a 10-h test.

The XANES approach required a series of rubbing tests of different duration to be carried out. In 2001, optical interferometry was adapted to measure the film thickness of ZDDP and other phosphorus-based antiwear films *in-situ* so that a series of film thickness measurements could be obtained from the same test [15]. The technique developed, MTM-SLIM, is described in the next section. This showed that ZDDP formed a rough, solid-like film that grew during rubbing to stabilize at a thickness of *ca* 100 nm. This film caused a marked increase in friction in the intermediate speed (mixed) lubrication regime; an effect that correlated with the thickness of the ZDDP film [16]. It was shown that this phenomenon originated because the ZDDP film inhibited fluid entrainment and thus delayed the formation of a separating hydrodynamic film to higher speed than in the absence of the ZDDP film [17]. Recently this optical interference technique has also been used to study the kinetics of ZDDP film formation and removal and the impact of other additives on ZDDP film thickness [18].

Since 1997, atomic force microscopy (AFM) has been widely used to study the morphology and physical properties of ZDDP-derived antiwear films [19–22]. Pidduck and Smith [19] studied ZDDP reaction films formed in a reciprocating Amsler test. AFM topography imaging revealed a typical morphology of long, smooth features or “pads”, aligned in the sliding directions interspersed by various densities of micron-sized pits. The dark areas (lower height) between the smooth pads were interpreted as areas where the antiwear film had either failed to form, or had been damaged. Root mean square surface roughness for pitted and pad regions over  $100\ \mu\text{m} \times 100\ \mu\text{m}$  areas was about 30 nm and 8 nm respectively. Pit depths were consistently found to be in the range of 100–140 nm. Although much AFM work has examined the topography of ZDDP films, little has been applied to determine the film thickness. This is

probably because of the difficulty of establishing a reference, zero thickness line against which the height of these films can be measured.

The aim of the work described in this article is to compare the two main methods for studying the thickness and roughness of ZDDP antiwear films, AFM and MTM-SLIM and thus both to determine typical values of these parameters for a range of ZDDPs and to identify the strengths and weaknesses of the two methods. A novel feature of the work is the use of an aqueous solution of a chelating agent to locally remove ZDDP film and thus provide a reference plane against which to determine film thickness.

## 2. Experimental

### 2.1. Test methods

Two main experimental techniques were employed in this study, MTM-SLIM and AFM. Both are briefly described below.

#### 2.1.1. MTM-SLIM method

Spacer layer interferometry imaging (SLIM) is an effective way of mapping lubricant films in elastohydrodynamic contacts [23]. The principle is shown in figure 1. A glass flat is loaded against a reflective steel ball. The surface of the glass in contact with the ball is coated with a thin, semi-reflective chromium layer, on top of which is a ‘spacer-layer’ of transparent silicon dioxide. When white light is shone into the contact, some of this light is reflected from the semi-reflective layer while some passes through the silicon dioxide layer and any lubricant film present on the ball before being reflected back from the steel surface. Since these two beams have travelled different distances, upon recombination they undergo optical interference, so that some component wavelength gain and some lose intensity, depending upon the optical path difference. The result is a coloured interference image of the contact and when this interference image is frame-grabbed by a colour

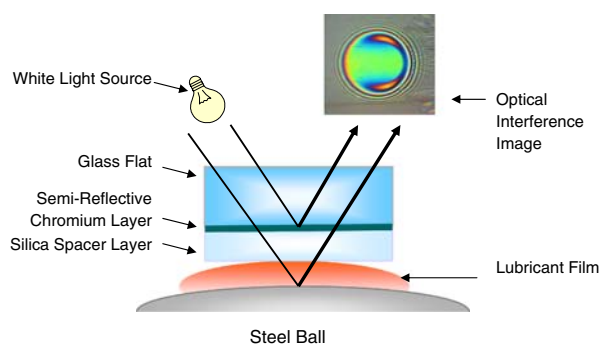


Figure 1. Principle of spacer layer interferometry.

camera, the red/blue/green colour of each pixel can be converted, *via* a suitable film thickness/colour calibration, into a map of path difference and thus of the film thickness separating the ball and the glass disc [22].

Spacer layer interferometry imaging is normally used to map the thickness of liquid lubricant films in rolling and rolling-sliding contacts. However ZDDP reaction films are only generated when direct, rubbing, solid contact occurs and such conditions abrade the spacer layer required for interferometry. This limitation has been overcome by applying spacer layer interferometry to study ZDDP reaction films on the stationary steel ball ‘*in situ*’ within a minitraction machine (MTM) tribometer, i.e. outside of the contact but within the rubbing test apparatus [15]. The test arrangement of the minitraction machine-spacer layer imaging method (MTM-SLIM) test-set up is shown in figure 2. The SLIM microscope is attached to a conventional MTM. The MTM-SLIM test protocol is briefly described below.

Prior to any rubbing, an optical interference image of the ball with no lubricant present is taken by loading a spacer layer-coated glass window against the ball and capturing an interference image. ZDDP solution is then added, the temperature is raised to the test value and a prolonged rolling-sliding is carried out. In this, the steel ball and steel disc are rubbed together in ZDDP solution at fixed, slow entrainment speed and thus in mixed lubrication conditions so as to generate a solid-like antiwear surface film on the ball and disc rubbing tracks. The total rubbing time in the current work was generally 4 h. Periodically throughout the test, motion is halted and an optical interference image is taken from the rubbed track on the ball using SLIM. This is done without any cooling or rinsing the ball (and hence *in-situ*). The measured optical film thickness is then converted to the true film thickness assuming that the film formed consists mainly of a phosphate glass with a refractive index of 1.60 [24]. A detailed description of MTM-SLIM experimental procedure can be found in Fujita and Spikes [25].

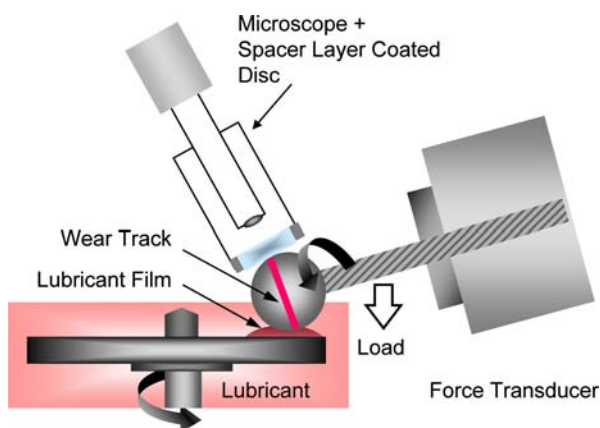


Figure 2. MTM-SLIM test set-up.

Table 1  
Base oil used.

Code	Description	Viscosity at 40 °C (m Pa s)	Viscosity at 100 °C (m Pa s)	VI
BO	Group II base oil	36.692	5.4376	108

Table 1 summarizes the conditions used for the MTM-SLIM tests in this study. The steel balls and discs used were both of AISI 52100 steel with hardness 750–770 VHN. The root mean square roughness,  $R_q$ , of both balls and discs was  $11 \pm 3$  nm, giving a composite surface roughness of  $\approx 16$  nm. Fresh ball and disc specimens were used for each test and these were cleaned prior to testing by successive immersion in toluene and isopropanol in an ultrasonic bath for 10 min. Throughout this study the test temperature was 100 °C and the applied load was 31 N, corresponding to an initial mean Hertz pressure of 0.95 GPa and a contact diameter of 250  $\mu\text{m}$ . The slide-roll ratio employed was 50%, where this is defined as the ratio of sliding speed  $u_s = (u_b - u_d)$  to the entrainment speed  $U = (u_b + u_d)/2$ , where  $u_b$  and  $u_d$  are respectively the speed of the ball and disc with respect to the contact.

### 2.1.2. AFM method

At the end of each 4-h MTM-SLIM test, the MTM discs were lightly rinsed in hexadecane and the ZDDP antiwear films formed on them were analysed using a Veeco Explorer AFM in contact mode. For better resolution, a Veeco liquid scanner was employed and samples were probed in *n*-hexadecane rather than air.

Two regions were scanned, one spanning the edge of a wear track and one close to the centre of the wear track. Typical scan area was 100  $\mu\text{m} \times 100 \mu\text{m}$ . Measured film thickness, topography and surface roughness data were obtained and compared with those from SLIM imaging. The film thickness was determined from scans which traversed the edge of the contact and the height of the non-rubbed region was used as a reference base line which was subtracted from the height within the wear track to provide the ZDDP film thickness, as shown schematically in figure 3(a). This approach makes two assumptions. One is that there is negligible wear of the metal surface below the ZDDP film within the wear scar. The second is that there is negligible ZDDP film outside of the wear track region. As illustrated schematically in figure 3(b), 3(c), both of these would result in the calculated film appearing thinner than it actually was.

### 2.1.3. AFM – EDTA Method

To address these two assumptions, AFM tests were carried out in which the ZDDP film was removed using a solution of EDTA. It is now well accepted that ZDDP reaction films formed on rubbing ferrous surfaces comprise a solid-like film which consists primarily of glassy



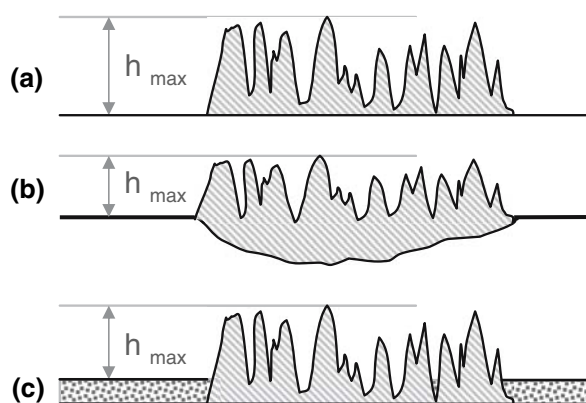


Figure 3. Schematic representation of the principle of the AFM maximum antiwear film thickness determination, (a) assuming negligible wear and film outside the wear track, (b) estimated film appearing thinner because of wear, (c) estimated film appearing thinner because of the presence of lubricant film outside the wear track.

phosphate based on Zn(II) and Fe(III) cations [26]. Ethylenediaminetetraacetic acid (EDTA) (and its disodium salt) is a chelating agent designed to form coordination complexes with most divalent and trivalent metal ions, including  $Zn^{2+}$  and  $Fe^{3+}$ , and thus appeared to be appropriate solvent for ZDDP film removal.

After ZDDP antiwear films had been analysed using AFM, a droplet of 0.05 M EDTA sodium salt solution in distilled water was deposited on the disc wear track using a micropipette and wiped off with the paper tissue after a set time. After some experimentation, a time of 1 min was found to be suitable. Areas where ZDDP film was removed were clearly seen visually within the wear track.

Table 2  
Additives tested.

Code	Description
ZDDP1	Primary ZDDP
ZDDP2A	Secondary c6 ZDDP
ZDDP2B	Secondary ZDDP
ZDDP2C	Secondary low volatility ZDDP
ZDDPar	Aryl ZDDP

These were characterized using the AFM in contact mode and also imaged with an optical microscope.

## 2.2. Test materials

A single base fluid was used throughout this study. This was a Group II mineral oil with viscometric properties listed in table 1.

Five different ZDDP additives were studied, as listed in table 2. All were commercial products, one a primary ZDDP, three secondary ZDDPs and one an aryl ZDDP. These were all tested individually at a concentration of 0.08 wt% P in base oil solution.

## 3. Results

### 3.1. MTM-SLIM results

Figure 4 shows series of optical interference images obtained during 4-h rubbing tests on all five ZDDP solutions. In all of these images the sliding direction is from left to right. The development of a patchy ZDDP

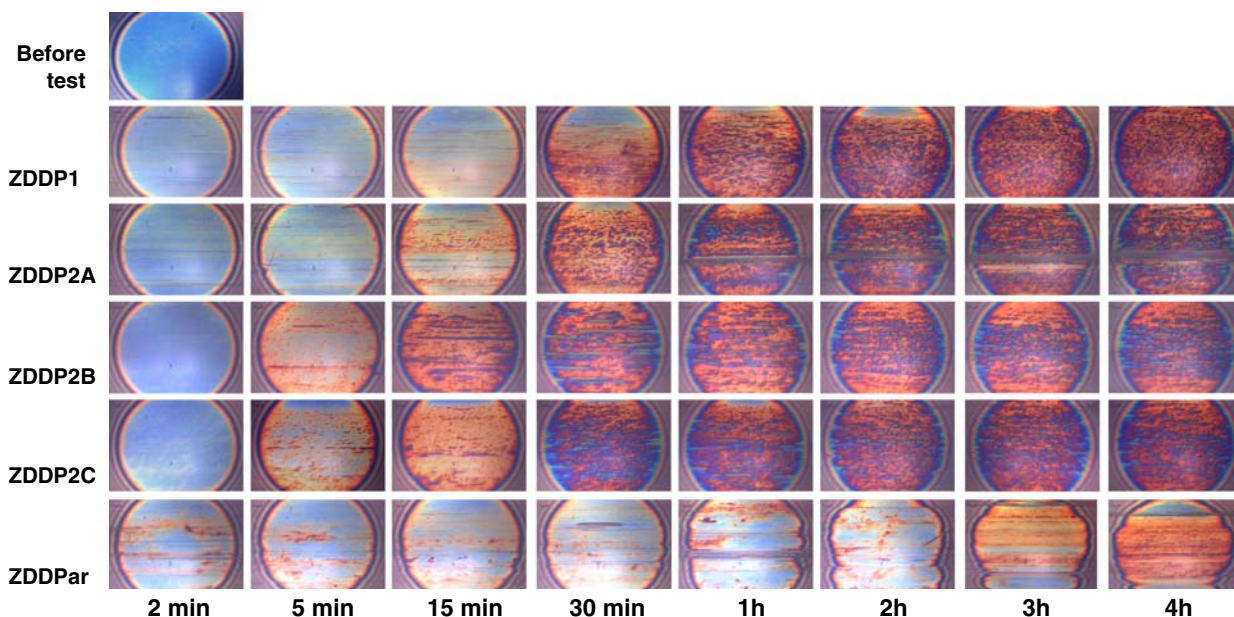


Figure 4. Series of interference images of the ball wear track of primary ZDDP1, secondary ZDDP2A, ZDDP2B and ZDDP2C, and aryl ZDDPar solutions in base oil at a concentration of 0.08% w/w, entrainment speed of 0.1 m/s, slide-roll ratio of 0.5 and temperature 100 °C. The circular, steel ball on glass disc contact regions shown in these images are 260  $\mu$ m in diameter.

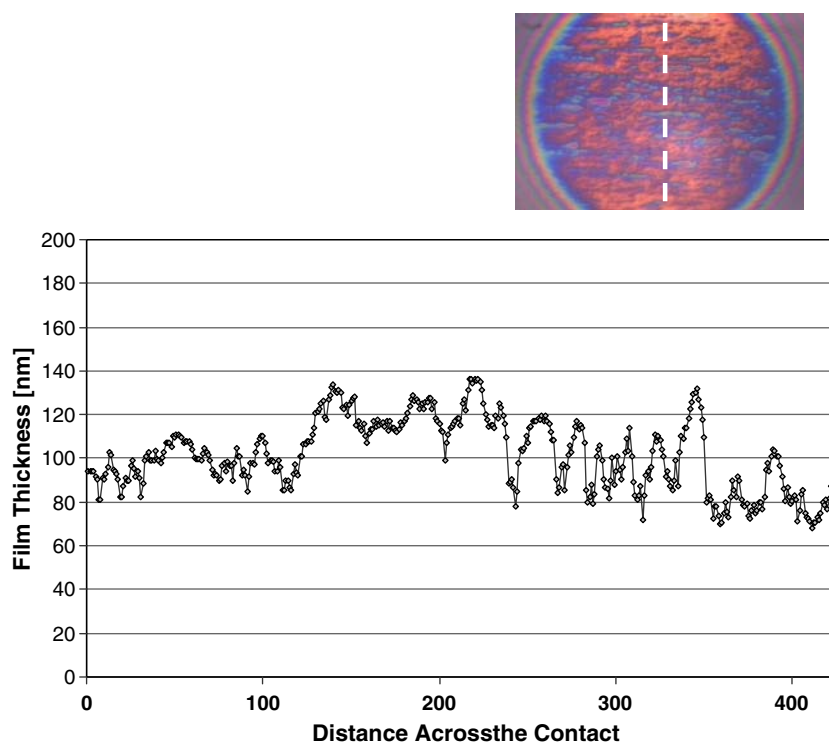


Figure 5. Interference image of the ball wear track and SLIM film thickness line profile across the MTM ball wear track of ZDDP2B solution after a 4-h MTM rubbing test.

antiwear reaction film on the wear track during rubbing, indicated by the dark areas within the contact, can be clearly seen. It can also be seen that for the four alkyl ZDDP solutions the reaction film develops rapidly – for the primary ZDDP slightly slower than the secondary ZDDPs. The aryl ZDDP solution only starts to form a thick film after 3 h rubbing. This is consistent with the findings of Yamaguchi et al. [27].

From these interference images, maps of film thickness were calculated and the average, maximum and root mean square variation of the ZDDP tribofilm thickness in the central region of each image were determined. A typical line profile of thickness calculated from a SLIM image is shown in figure 5.

Film thicknesses of all five ZDDP solutions are compared in figure 6. Considering mean film thickness (figure 6(a)), the four alkyl ZDDP solutions show quite similar behaviour, all exhibiting rapid film growth over the first 30 min rubbing, after which the film thickness stabilizes. At the end of the test all four form a similar mean film thickness of 100 nm. However a few minor differences can be observed. The ZDDP2B solution exhibits the fastest growth, while ZDDP2A film growth is slower and reaches a maximum value only after 1 hour of rubbing. The film growth of the aryl ZDDP solution is significantly different. Mean film thickness shows only moderate increase for up to 2 h rubbing, after which the mean film thickness starts to rise to reach 80 nm at the end of the 4-h rubbing test, but without having stabilised at a constant value.

As shown in figure 6(b), for the alkyl ZDDPs the maximum film thickness is typically about 20–50% higher than the mean value. For the aryl ZDDP however,

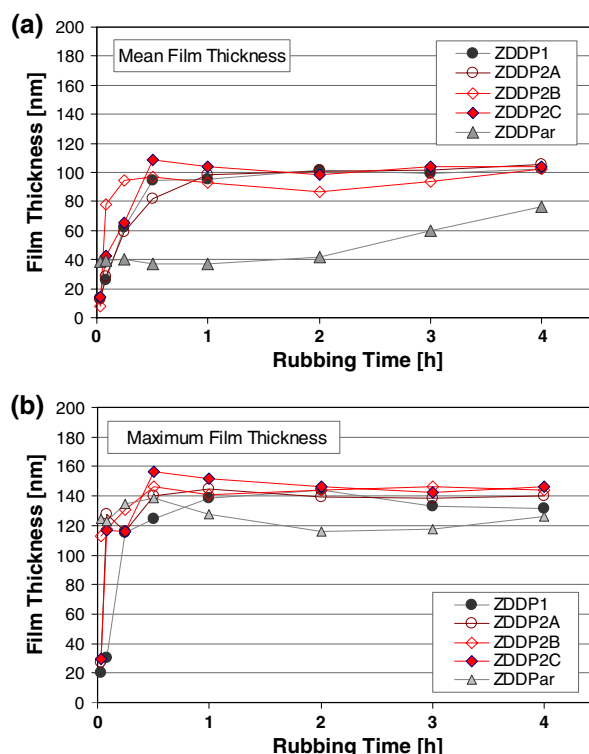


Figure 6. (a) Mean and (b) maximum film thickness with rubbing time for five ZDDP solutions.

maximum film thickness increases much more rapidly than mean thickness, at a comparable rate to the alkyl ZDDPs. At the end of the 4-h tests, the three secondary ZDDP solutions show very similar maximum film thickness of 140 nm, the primary ZDDP solution gives 130 nm and aryl ZDDP solution 120 nm.

Figure 7 shows the root mean square (rms) values of the thickness of the ZDDP antiwear films developed during 4-h MTM rubbing tests. These can be considered to represent the roughness of the films. For clarity, the five ZDDP solutions are shown in two figures. As can be seen from figure 7(a), the films formed by the three secondary ZDDPs show similar rms behaviour. The rms stabilizes at a value of between 15 nm and 20 nm within 30 min rubbing. At the end of the 4-h test all three secondary ZDDP films have very similar SLIM rms values of around 15 nm. The rms of the antiwear film derived from the primary ZDDP solution (figure 7(b)) shows a large variation in rms in the first half hour of the test, after which rms slowly reduces to reach a value of 10 nm at the end of the test. The rms of the aryl ZDDP solution-derived antiwear film shows the biggest variation throughout the 4-h test, with initial values up to 30 nm, falling to 20 nm at the end of the test.

### 3.2. AFM results

At the end of the 4-h MTM-SLIM tests, the MTM discs were rinsed in hexadecane and the tribofilms were

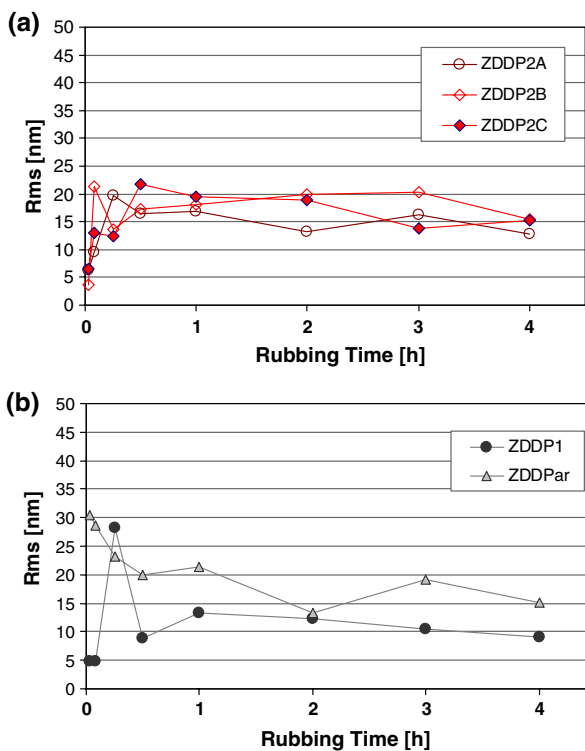


Figure 7. Variation of SLIM rms surface roughness of reaction films with rubbing time (a) secondary ZDDP and (b) primary and aryl ZDDP solutions.

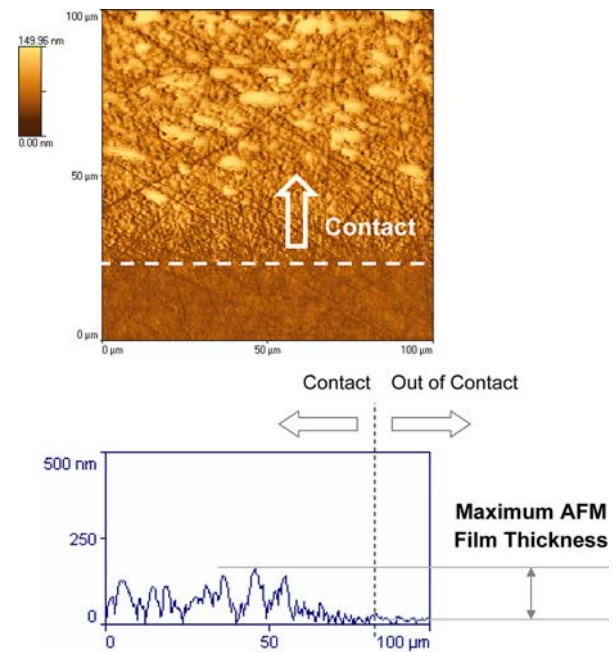


Figure 8. AFM topography image and profile across the edge of the wear track on the steel disc after 4 h test using ZDDP2B solution. The dashed line on image marks the edge of contact track. The profile is taken from the top to the bottom of the image.

analysed using AFM. In order to determine the film thickness, an area of  $100 \mu\text{m} \times 100 \mu\text{m}$  was scanned at the edge of the wear scar. A line profile was taken in the direction perpendicular to the sliding direction. It was initially assumed that no significant film was formed outside the rubbing contact and that the height difference between the level outside the wear track and the highest point in the wear track represents the maximum film thickness of the ZDDP solution derived antiwear film. This lack of a significant thermal film is confirmed in section 3.4 later in this article. Figure 8 shows a typical profile spanning the edge of the rubbing track from a test using ZDDP2B solution.

The maximum film thickness of tribofilms formed by the five ZDDP solutions is compared in figure 9. As can be seen, ZDDP2C solution, with film thickness 150 nm,

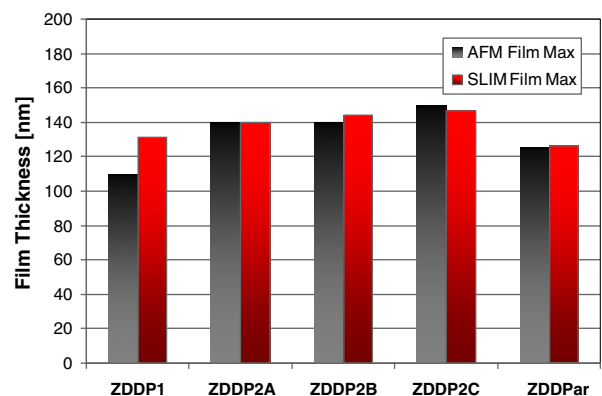


Figure 9. Comparison of SLIM and AFM maximum film thickness of antiwear formed by five ZDDP solutions in 4-h MTM rubbing tests.

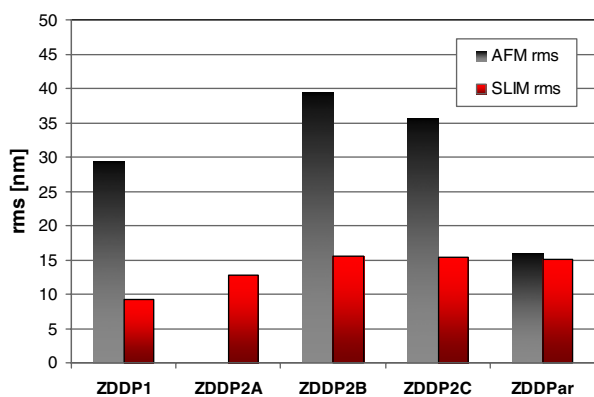


Figure 10. Comparison of SLIM and AFM rms values of antiwear film formed by five ZDDP solutions in 4-h MTM rubbing tests.

exhibits the highest film maximum thickness and ZDDP1 solution, with maximum film thickness of 110 nm, forms the thinnest film.

For all three secondary ZDDP and the aryl ZDDP solution the maximum film thickness data obtained using the two different methods, SLIM and AFM, are almost identical. The only significant difference is observed from the primary ZDDP1 solution, where the maximum film thickness value obtained with SLIM is about 20% higher than the value obtained with the AFM. It should be noted that SLIM data were obtained from the wear track on the MTM ball, while the AFM data were obtained from the MTM disc, both taken from the very same experiment. This was because a ball geometry is more difficult to study using AFM than a flat surface. However a test carried out in which AFM was applied to both the rubbed ball and disc showed negligible difference between the ZDDP films on the two surfaces.

Using the AFM, areas in the centre of the wear track were also scanned and rms values were obtained from these. Figure 10 compares the rms values of ZDDP antiwear films produced in the 4-h MTM rubbing test as measured by the two methods, SLIM and AFM, respectively.

It can be seen that SLIM and AFM rms values differ significantly, AFM generally giving much higher values than the SLIM method. The only exception is for the aryl ZDDP solution-derived tribofilm, where SLIM rms is similar to AFM rms. The likely reason for these differences will be discussed later in this article.

### 3.3. Wear results

Wear track width (WSW) was measured from the MTM disc after the 4-h MTM rubbing test using an optical microscope. Figure 11 compares film thickness and wear scar width for all five ZDDP solutions tested.

Overall, it can be seen that the formation of a thicker film generally correlates with a narrower wear track,

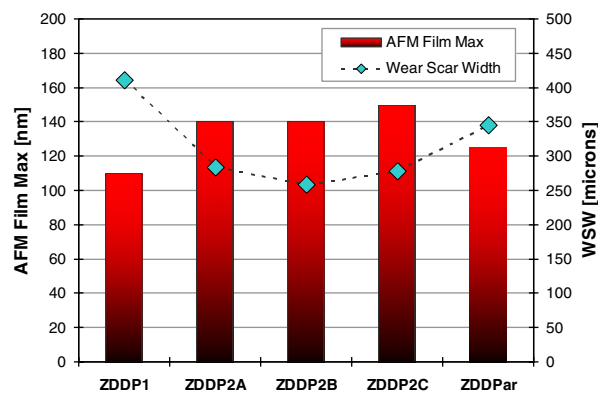


Figure 11. AFM maximum film thickness and wear scar width from the antiwear film formed by five ZDDP solutions on the MTM disc after 4-h rubbing tests.

with secondary ZDDP solutions exhibiting the highest film thickness and lowest WSW and the primary ZDDP with the lowest maximum film thickness showing the widest WSW. In order to investigate the wear properties further and help understand the difference between SLIM and AFM measurements, antiwear films were partially removed using EDTA and the wear tracks 'underneath' these film were examined using optical microscope and AFM imaging.

### 3.4. EDTA results

Figure 12 shows optical microscope images of disc wear tracks from a 4 h MTM rubbing test after local film removal using EDTA. All images are the same magnification, confirming figure 11, that ZDDP1 exhibits the largest wear scar width and ZDDP2B the smallest.

The region where the EDTA droplet was deposited and film removed can be clearly seen in the lower half of each image. For the four alkyl ZDDP solutions this region appears brighter than the out-of-track area where no EDTA was deposited, with the interface being clearly visible. Tests with EDTA deposited on a new, non-rubbed steel MTM disc revealed no significant visible difference between areas where EDTA was deposited for up to 3 min compared to the steel surface outside these areas. This suggests that, for the four ZDDP solutions where a clear difference in brightness outside of the wear scar can be observed after EDTA film removal process, there is a thin thermal ZDDP film formed outside the wear scar which is removed by the EDTA. From the optical microscope image of the aryl ZDDP no such effect is seen, suggesting that this ZDDP forms no thermal film during tests.

For the additive ZDDP2B, the region inside the wear track where the ZDDP film is removed shows almost no evidence of wear. Polishing marks are still visible and all the film seems to be removed by the EDTA, suggesting



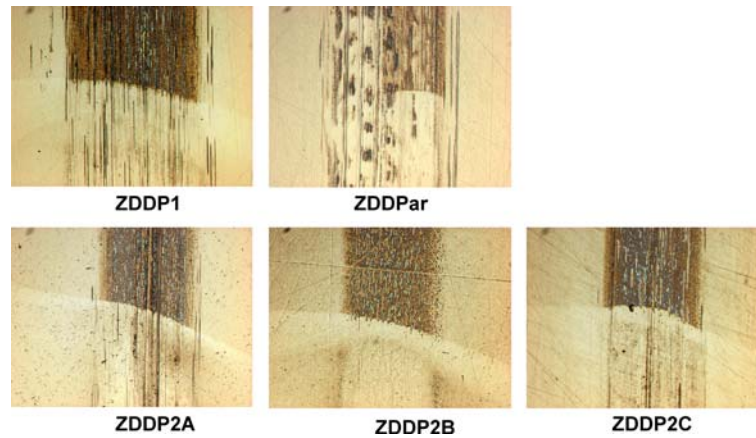


Figure 12. Optical microscope images of the edge of the wear scar from the antiwear film formed by five ZDDP solutions on MTM discs after 4-h rubbing tests and after the antiwear films were locally removed with EDTA. All microscope images are the same magnification.

that it was essentially all phosphate glass. The primary ZDDP shows many wear scratches oriented in the sliding direction. Some of these appear darker in colour suggesting that a film is still present, which thus may not be phosphate glass. For the aryl ZDDP, no polishing marks after film removal can be seen and a significant amount of wear scarring appears in the wear track. Also dark patches of a film formed are visible which could not be removed by the EDTA. Considerable wear can also be observed for two secondary ZDDP solutions, ZDDP2A and ZDDP2C, respectively.

Overall it can be seen that the optically-visible wear observed after ZDDP film removal by EDTA correlates

well with the wear scar diameter, the bigger the WSW, the more wear scarring is observed in the rubbed area. However correlation with the film thickness is not as straightforward. For example, ZDDP2C, which exhibits the highest film thickness of 150 nm exhibits significant more wear than ZDDP2B, which has a maximum ZDDP film thickness of 140 nm.

Regions where ZDDP film was removed by EDTA were also scanned using AFM. Figures 13, 14 present AFM topography scans of these regions. Scanning was performed at the edge of the wear scars, so that areas of rubbed surfaces could be compared to the unrubbed steel surface. As can be seen, the unrubbed steel surfaces

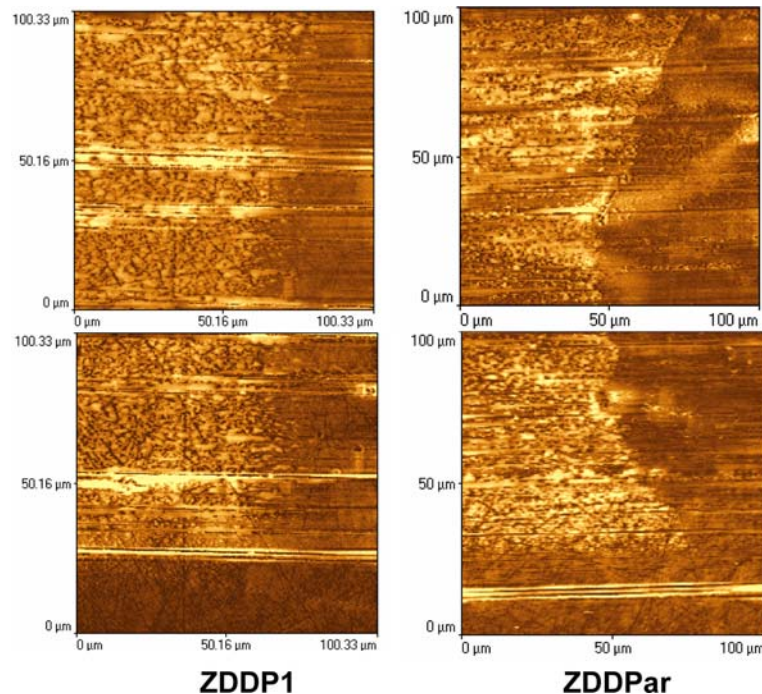


Figure 13. AFM topography images of the edge (lower images) and the centre (upper images) of the wear scar after EDTA film removal of films formed by primary and aryl ZDDP solutions in 4-h MTM rubbing tests on MTM discs. Sliding direction of all images is from left to right.



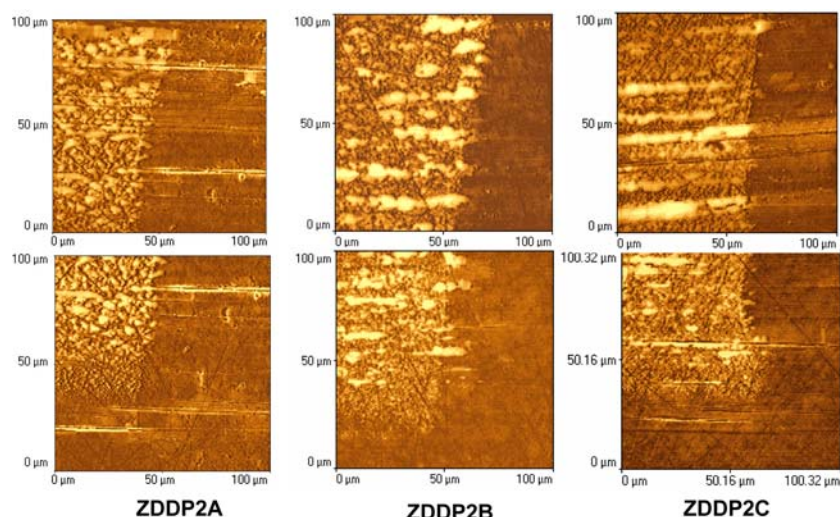


Figure 14. AFM topography images of the edge (lower images) and the centre (upper images) of the wear scar after EDTA film removal of films formed by three secondary ZDDP solutions in 4-h MTM rubbing tests on MTM discs. Sliding direction of all images is from left to right.

show polishing marks. After film removal, polishing marks are also clearly visible within the rubbing tracks from tests on all ZDDP solutions. These are less visible for the primary and aryl ZDDP (figure 12) inside the wear track. Wear scars, visible as tiny dark lines elongated in the sliding direction, are visible for these two ZDDPs and also two of the secondary ZDDPs, ZDDP2A and ZDDP2C respectively, indicating that some wear occurred during the rubbing test. These wear scars are approximately 6–15 nm deep. For the ZDDP2B solution there is no significant difference between the unrubbed steel surface outside the wear track and in the rubbing contact 'beneath' the antiwear film.

Atomic force microscopy topography revealed no step in the out-of-contact region due to a thermal film, as could be seen in the optical microscope images (Figure 12), indicating that any possible thermal film formed was thinner than the AFM detection limit (2 nm). Spacer layer imaging of the ball outside the wear track also confirmed that any thermal film, if present,

was less than 5 nm thick. However, lateral force imaging showed the presence of lower lateral force in the out-of-track, EDTA-treated region than the out-of-track, non-EDTA-treated surface, suggesting either that a ZDDP film was present outside the rubbing track, albeit extremely thin, or that the EDTA had removed some other, non-ZDDP based film (figure 15).

Previous work using SLIM showed that a secondary ZDDP gave negligible thermal film formation over 12 h at 80 °C although film formation was more rapid at 150 °C [25], while XANES showed formation of a thermal film only 11 nm thick after 8 h immersion in a secondary ZDDP solution at 145 °C [13]. This supports the observation that measurable thermal films were not formed at the conditions used in this study.

Figure 16 shows two SLIM interference images taken by loading the coated glass disc against the wear track on the steel ball from a 2-h ZDDP2B test after EDTA treatment. The image on the right is from the edge of the EDTA droplet and non-removed ZDDP film that lies

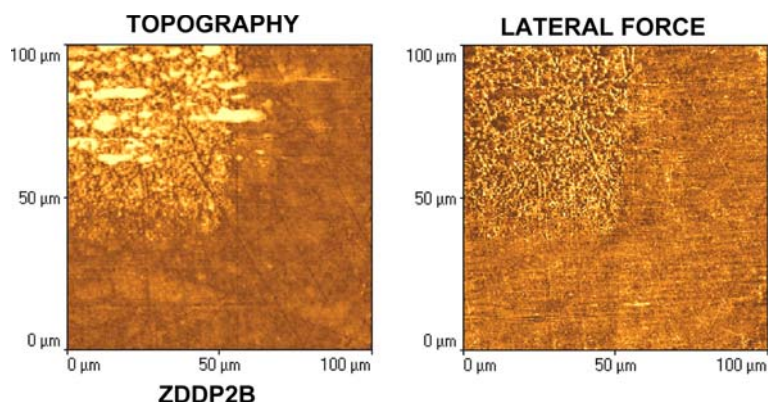


Figure 15. AFM topography and lateral force image of the edge of the wear scar after EDTA film removal of ZDDP2B solution reaction film.

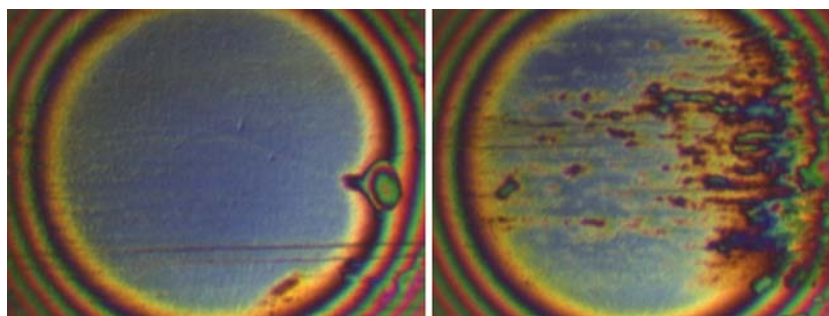


Figure 16. SLIM images from the ball wear track after EDTA film removal. The right-hand image is at the edge of the EDTA-treated zone while the left-hand one is from the middle of the EDTA-treated region.

outside the EDTA droplet can be seen on the right of this image. The left-hand image is from well inside the EDTA-treated region. There is no significant film ( $< 5$  nm) present, confirming the AFM results, that EDTA removes essentially all of the film.

#### 4. Discussion

In terms of the maximum film thickness of ZDDP film it can be seen that there is quite good agreement between measurements made by the SLIM and the AFM methods. Indeed, considering the fact that the refractive index value of 1.6 used in the MTM-SLIM is an approximate one, the agreement is surprisingly close.

There is, however, a large difference in the measured roughness of the film, with AFM showing much rougher films than SLIM. The most likely reason for this is that SLIM fails to identify the presence of deep valleys in the ZDDP reaction film. From the AFM images and the profile in figure 8, it is clear that the reaction film pads are separated by deep fissures, where the film thickness falls to practically zero. However, as shown in the profile in figure 5, the SLIM images show only shallow valleys. This is probably because the glass disc, which is pressed against the ball to capture an interference image, is not elastic enough to fully conform to the very deep valleys. Also if the valleys in the ZDDP film are full of liquid lubricant the latter may be trapped by the glass disc and maintain a separation even if the glass could, in principle, elastically conform to the dry ZDDP film topography.

This is an important difference because one of the most likely reasons why ZDDP films increase mixed friction is that the deep valleys serve as drainage paths in the contact inlet and prevent the build-up of fluid pressure inlet, thereby inhibiting the entrainment of an elastohydrodynamic lubricant film. This may be why friction increases with the thickness of the ZDDP film – because a thicker film means deeper valleys. If this is the case then it must be studied by AFM rather than SLIM.

The results show that there are significant differences not just between the aryl, primary and secondary

ZDDPs but also between the individual secondary ones. Thus ZDDP2B shows less wear than the other two secondaries. From figure 6 it can be seen that this additive forms a “full” film – i.e. one with a high mean film thickness – considerably more rapidly than the other two. In these 4-h tests most of the observed wear probably takes place in the rubbing period while the film is formed, and this probably explains why ZDDP2B is so effective in reducing wear.

The use of EDTA to remove the ZDDP films appears to be a very effective tool for learning more about the film. In the current study it confirms (i) that there is very little removal of steel below the ZDDP in the current tests – only isolated wear grooves of less than 15 nm depth – and (ii) that the thermal film formed outside the wear track is always  $< 2$  nm thick. This validates the use of an AFM profile across the side of the rubbing track as a method of measuring the thickness of the ZDDP film.

It should be noted that while the AFM and optical techniques used in the current study show that the EDTA treatment removes almost all of the ZDDP reaction film present, they are not sufficiently sensitive to confirm that all of this film has gone. The continued presence of residual material up to a couple of nanometers thick, perhaps of components insoluble in EDTA, cannot be excluded. Surface sensitive analysis techniques such as XPS could be applied to resolve this issue in future work.

#### 5. Conclusions

Space layer interferometry imaging and atomic force microscopy have been employed to measure the film thickness and roughness of surface films formed by ZDDP solutions in rolling-sliding, steel-on-steel contact. A novel technique based on the use of EDTA solution to remove locally the ZDDP reaction film has been developed to confirm the validity of the AFM film thickness measurements. Both measurement techniques show that alkyl ZDDPs form films which stabilize at *ca* 150 nm maximum thickness after extended rubbing in the test conditions used. However the AFM method determines

much rougher films than SLIM. This is probably because the SLIM method does not penetrate deep valleys present in the ZDDP reaction film and thus underestimates the film roughness.

Based on this study it is clear that both techniques have strengths and weaknesses and it is important that the researcher recognizes these. AFM is well-suited to study the morphology of ZDDP reaction films (and presumably other antiwear films) but SLIM is not. AFM is thus likely to be more useful when seeking to understand the origins of the high mixed friction exhibited by ZDDP.

Both techniques are able to measure film thickness with reasonable accuracy. However, AFM can only be employed at the end of a rubbing test while MTM-SLIM is able to monitor the evolution of film thickness throughout a test. Thus MTM-SLIM can be used to study the rate of film growth and removal and the effect of test conditions and lubricant formulation on these. It is thus arguably a more useful experimental technique than AFM for this type of study.

## References

- [1] L Taylor and H.A. Spikes, *Tribol. Trans.* 46 (2003) 303.
- [2] J.M. Palacios, *Wear* 114 (1987) 41.
- [3] E.H. Loeser, R. Wiquist and S. Twiss, *ASLE Trans.* 1 (1958) 329.
- [4] F.G. Rounds, *ASLE Trans.* 7 (1964) 11.
- [5] J.M. Georges, J.M. Martin, T. Mathia, Ph. Kapsa, G. Meille and H. Montes, *Wear* 53 (1979) 9.
- [6] A. Tonck, J.M. Martin, Ph. Kapsa and J.M. Georges, *Tribol. Int.* 12 (1979) 209.
- [7] A.F. Alliston-Greiner, J.A. Greenwood, A. Cameron, *Proc. Inst. Mech. Eng. Intern. Conf. Tribology, Friction, Lubrication and Wear, Fifty Years On*, 565–572 1987.
- [8] H So and Y.C. Lin, *Wear* 177 (1994) 105.
- [9] E.S. Yamaguchi, P.R. Ryason, S.W. Yeh and T.P. Hansen, *Tribol. Trans.* 41 (1998) 262.
- [10] H Gao, J.S. McQueen, E.D. Black, A.K. Gangopadhyay and R.K. Jensen, *Tribol. Trans.* 47 (2004) 200.
- [11] J.M. Palacios, *Tribol. Intern.* 19 (1986) 35.
- [12] S.H. Choa, K.C. Ludema, G.E. Potter, B.M. De Koven, T.A. Morgan and K.K. Kar, *Wear* 177 (1994) 33.
- [13] M.L. Suominen Fuller, L. Rodriguez Fernandez, G.R. Massoumi, W.N. Lennard, M. Kasrai and G.M. Bancroft, *Tribol. Lett.* 8 (2000) 187.
- [14] Z Zhang, E.S. Yamaguchi, M. Kasrai and G.M. Bancroft, *Tribol. Lett.* 19 (2005) 211.
- [15] L. Taylor, R. Glovnea, M. Ribeaud, H.A. Spikes, *Proc. Intern. Tribology Conf. Nagasaki, 1257–1262 2000*, 2, JST Tokyo, (2001).
- [16] L.J. Taylor, *The Film-Forming and Wear-Reducing Properties of Antiwear Additives*, PhD Thesis (University of London, April 2001).
- [17] L Taylor and H.A. Spikes, *Tribol. Trans.* 46 (2003) 310.
- [18] H Fujita, R.P. Glovnea and H.A. Spikes, *Tribol. Trans* 48 (2005) 558.
- [19] A.J. Pidduck and G.C. Smith, *Wear* 212 (1997) 254.
- [20] J.F. Graham, C. McCague and P.R. Norton, *Tribol. Lett* 6 (1999) 149.
- [21] M Aktary, M.T. McDermott and G.A. McAlpine, *Tribol. Lett* 12 (2002) 155.
- [22] K Topolovec-Miklozic and H.A. Spikes, *Trans. ASME J. Tribol.* 127 (2005) 405.
- [23] P.M. Cann, J. Hutchinson and H.A. Spikes, *Tribol. Trans* 39 (1996) 915.
- [24] R.K. Brow, D.R. Tallant, S.T. Myres and C.C. Phifer, *J. Non-Crystalline Solids* 191 (1995) 45.
- [25] H Fujita and H.A. Spikes, *Proc. Inst. Mech. Eng J218 (277)* 265.
- [26] J.M. Martin, C. Grossiord, T. Le Mogne, S. Bec and A. Tonck, *Tribol. Intern.* 34 (2001) 523.
- [27] E.S. Yamaguchi, P.R. Ryason and T.P. Hansen, *Trib. Lett.* 3 (1997) 27.